Supporting Information:

Oxygen Evolution Activity on NiOOH catalysts: Four-Coordinated Ni Cation as Active Site and Hydroperoxide mechanism

Li-Fen Li, Ye-Fei Li* and Zhi-Pan Liu*

Collaborative Innovation Center of Chemistry for Energy Material, Key Laboratory of Computational Physical Science (Ministry of Education), Shanghai Key Laboratory of Molecular Catalysis and Innovative Materials, Department of Chemistry, Fudan University, Shanghai 200433, China

*Email: yefeil@fudan.edu.cn zpliu@fudan.edu.cn

1. Calculation Details for Theoretical Overpotential using CHE Approach

To calculate the OER overpotential, we use the Standard Hydrogen Electrode (SHE: $H^+ + e^- \rightarrow 1/2H_2$, pH = 0, p = 1 bar, T = 298.15K) as reference, where we get

$$\Delta G = 1/2G^o[H_2] - \mu[H^+] - \mu[e^-]^{SHE} = 0 \qquad (1)$$

where $G^o[H_2]$ is the Gibbs free energy of H_2 in the standard condition; $\mu[H^+]$ the electrochemical potential of proton; $\mu[e^-]^{SHE}$ the electrochemical potential of electron in SHE. $\mu[H^+]$ can be estimated as

$$\mu[H^+] = 1/2G^o[H_2] - \mu[e^-]^{SHE} \qquad (2)$$

Using Eq. 2, we can derive the ΔG of an electrochemical half-reaction as described by formula 3.

$$HA \rightarrow A + H^+ + e^- \qquad (3)$$

The ΔG is given by

$$\Delta G = G[A] + \mu[H^+] + \mu[e^-] - G[HA] \qquad (4)$$

Substituting Eq. 2 into Eq. 4, we get

$$\Delta G = G[A] + 1/2G^o[H_2] - \mu[e^-]^{SHE} + \mu[e^-] - G[HA]$$
$$= G[A] + 1/2G^o[H_2] - G[HA] + (\mu[e^-] - \mu[e^-]^{SHE})$$
$$= G[A] + 1/2G^o[H_2] - G[HA] - |e|U \qquad (5)$$

U is the electrode potential relative to SHE and is given by

$$U = (\mu[e^-]^{SHE} - \mu[e^-])/e \qquad (6)$$

Setting $\Delta G = 0$, U is the standard electrode potential for half-reaction of $HA \rightarrow A + H^+ + e^-$. The theoretical overpotential then be calculated by Eq. 7.

$$\eta = U - 1.23 \text{ V} \qquad (7)$$

where 1.23 V is the standard electrode potential of OER.

2. Calculation Details for the Free Energy of Dissolved Cations

As we have shown in the main text, the formation free energy (ΔG_{vac}) is defined as

$$*(oxide) + 3H^+(aq) + e^- \rightarrow *\square\text{-3H}(oxide) + Ni^{2+}(aq) \qquad (8)$$
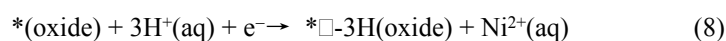
and

$$\Delta G_{vac} = \mu[Ni^{2+}(aq)] + G(*\square\text{-3H}) - G(*) - 3\mu[H^+(aq)] - \mu[e^-] \qquad (9)$$

*□ represents a cationic vacancy on γ-NiOOH surface. To estimate ΔG_{vac}, it is essential to calculate the electrochemical potential $\mu[Ni^{2+}(aq)]$. To this end, we use the standard half-electrode potential $E^0(Ni(s)/Ni^{2+})$

$$Ni(s) \rightarrow Ni^{2+} + 2e^- \tag{9}$$

and

$$G^0[Ni(s)] = \mu[Ni^{2+}(aq)] + 2\mu[e^-] = \mu[Ni^{2+}(aq)] - 2eE^0(Ni(s)/Ni^{2+}) \tag{10}$$

With Eq. 10, $\mu[Ni^{2+}(aq)]$ can be derived from the $G^0[Ni(s)]$ and $E^0(Ni(s)/Ni^{2+})$. The contribution of $c[Ni^{2+}]$ can be further corrected by a term of $0.059*\log(c[M^{2+}])$. It should be noticed that PBE+U cannot correctly describe the free energy of metals, e.g. Ni(s). To avoid directly calculate the energy of Ni(s), we further use the standard molar Gibbs energy of formation of $Ni(OH)_2(s)$ to derive the free energy of Ni(s).

$$\Delta_f G^0(Ni(OH)_2(s)) = G^0(Ni(OH)_2(s)) - G^0(Ni(s)) - G^0(H_2) - G^0(O_2) \tag{11}$$

In addition, the binding of O_2 molecule in PBE is overestimated. We derive $G^0(O_2)$ from $G^0(O_2) = \Delta_f G^0(H_2O) + 2G^0(H_2O) - 2G^0(H_2)$. The approach to correct the free energy of O_2 has been widely used in previous literature.[1-8]
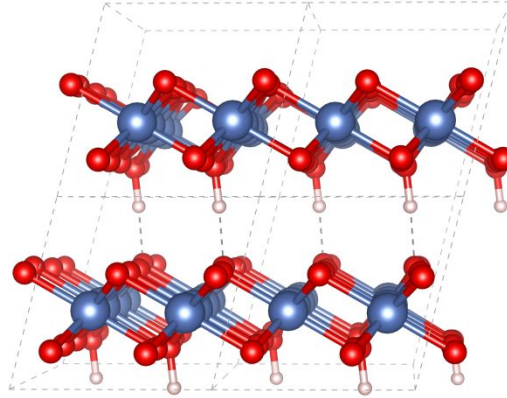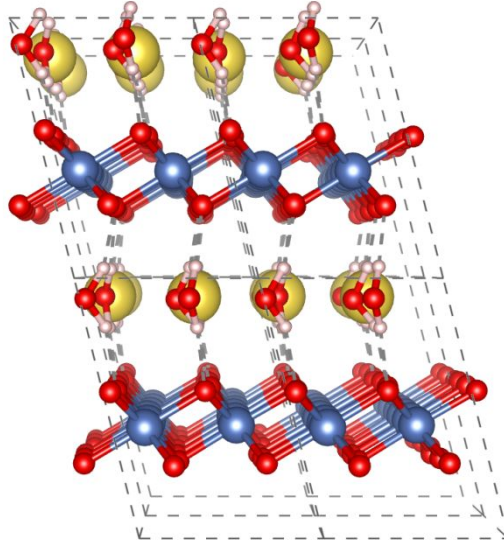

Figure S1. Crystal structure of deprotonating β-NiOOH.

Figure S2. Proposed crystal structure of γ-NiOOH intercalated with Na^+ and H_2O.

Table 1. Surface energies of γ-NiOOH

(hkil)	$\gamma(J/m^2)$
0001	0.277
$01\bar{1}2$	0.311
0110	0.533
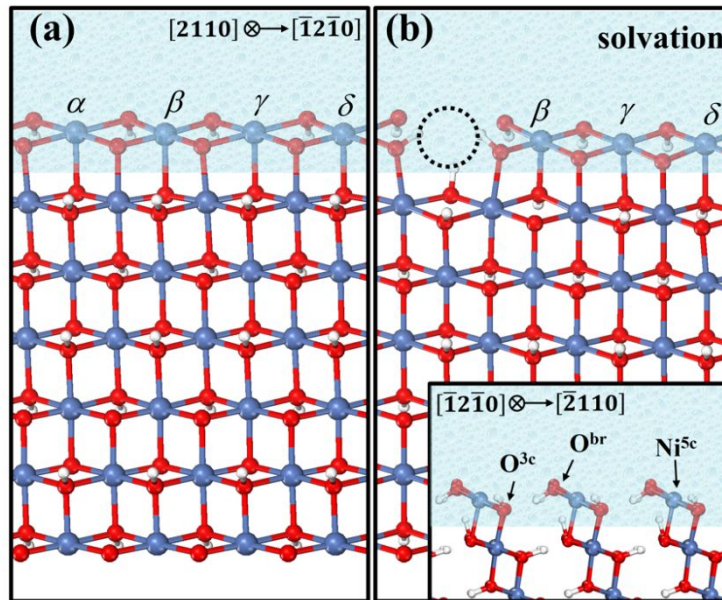
Figure S3. Overview of (a) pristine and (b) defective β-NiOOH ($01\bar{1}2$) surfaces. The black dotted cycle highlights the cationic vacancy in the first Ni layer. We label the four reactive Ni sites in the unit cell as α, β, γ, δ, respectively. Ni^{5c} represents five-coordinated Ni cation; O^{br} the bridging O anion; O^{3c} the three-coordinated O anion. Indigo balls: Ni; Red balls: O; White balls: H.
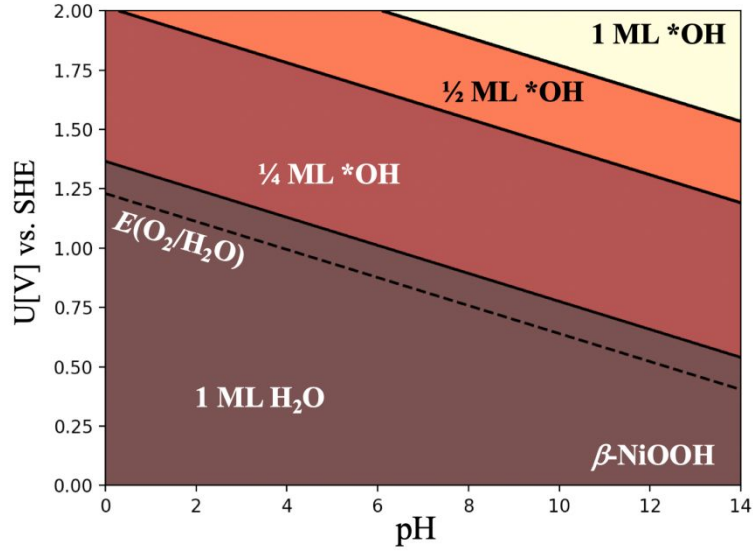
Figure S4. Surface Pourbaix diagram for the pristine β-NiOOH ($01\bar{1}2$). U is the electrode potential relative to SHE. The oblique dashed line represents the reversible potential of OER.
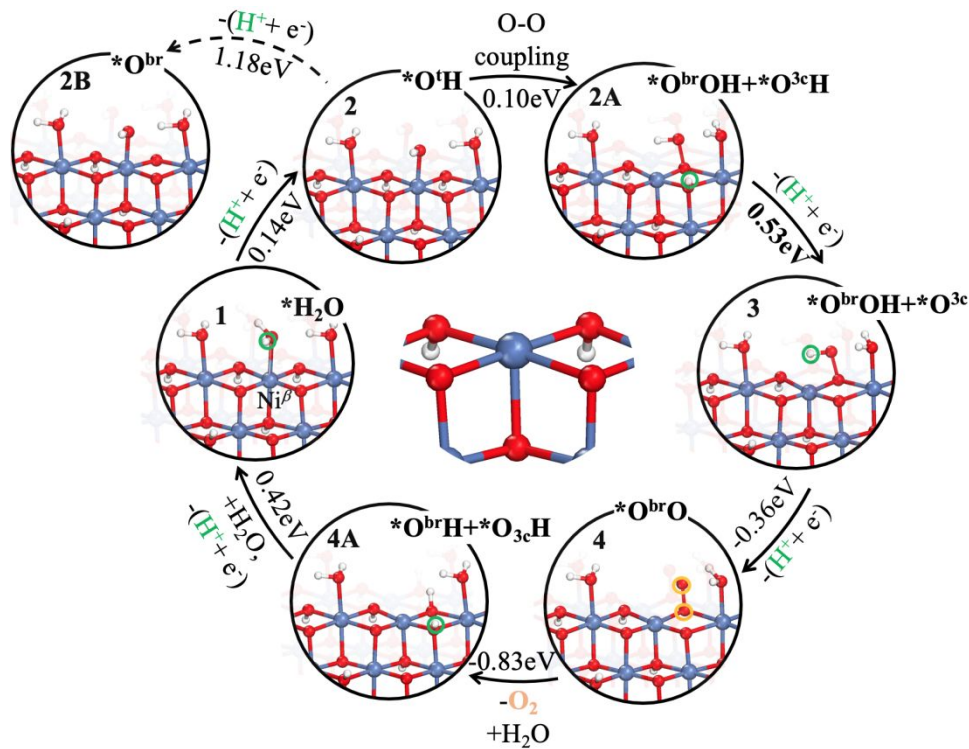
Figure S5. Reaction network for OER on pristine β-NiOOH ($01\bar{1}2$). The solid path denotes the mechanism of OER, where state 1 is the initial state. The end-on dashed path indicates this pathway is blocked due to the high free energy cost. The small green or yellow cycles highlight the proton or O_2 that would release from the surface in the subsequent step. The translucent atoms belong to the adjacent NiOOH layer. The energy aside each arrow represents the corresponding free energy change by PBE+U. The bold free energy change indicates this step is rate-determining. The local environment of the reactive Ni^{5c} site is highlighted in the center of the figure. Indigo balls: Ni; Red balls: O; White balls: H.
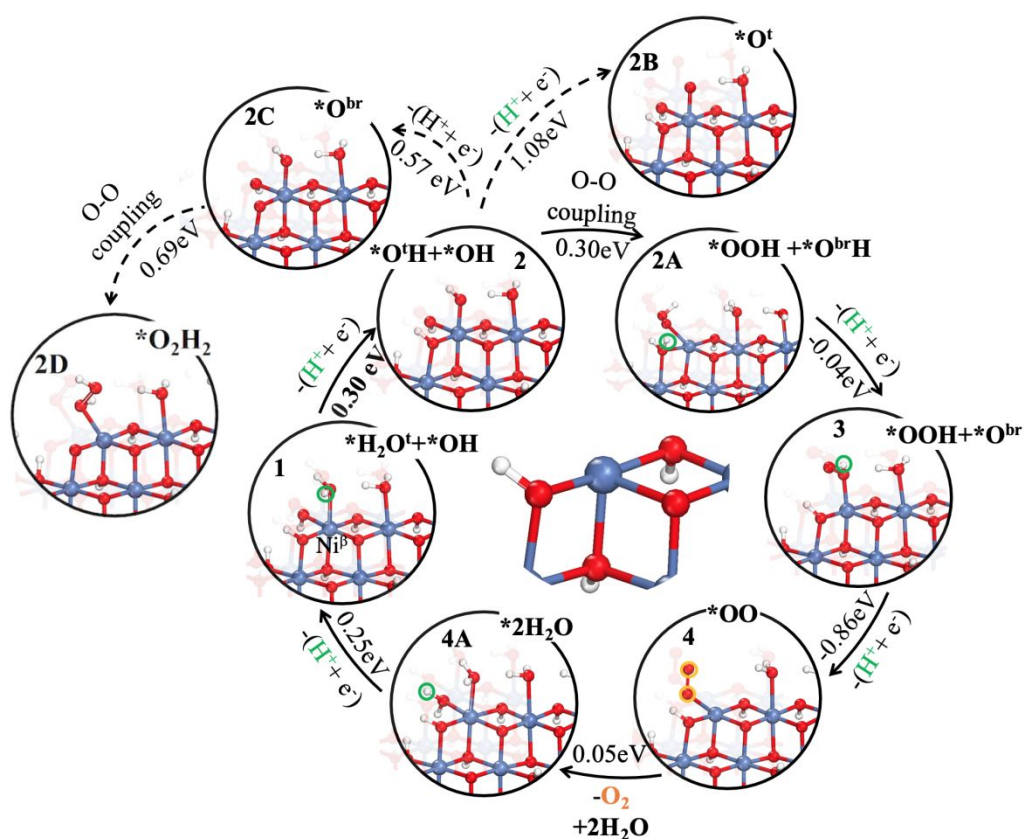
Figure S6. Reaction network for OER on the defective β-NiOOH. The solid path denotes the mechanism of OER on the defective β-NiOOH, where state 1 is the initial state. The end-on dashed path indicates this pathway is blocked due to the high free energy cost. The small green and yellow cycles highlight the proton or O_2 that would release from the surface in the subsequent step. The translucent atoms belong to the adjacent NiOOH layer. The chemical formula and the energy aside on the arrow represent the variation of the chemical composition and the corresponding free energy change by PBE+U. The bold free energy change indicates this step is rate-determining. The local environment of the reactive Ni^{4c} is highlighted in the center of the figure. Indigo balls: Ni; Red balls: O; White balls: H.

Table S2. Free energy changes (ΔG, in eV) of each elementary step by PBE+U and HSE06 functionals.

Elementary step	$\Delta G_{\text{PBE+U}}$ (ΔG_{HSE06})	$\Delta E_{\text{PBE+U}}{}^{\ddagger}$
pristine		
1→2: $*H_2O \to *O^tH + H^+(aq) + e^-$	0.14(0.07)	1.74
2→2A: $*OH^t + *O^{br}H + *O_{3c} \to *O^{br}OH + *O_{3c}H$	0.10(-0.17)	0.03
2A→3: $*O^{3c}H \to *O^{3c} + H^+(aq) + e^-$	**0.53(0.93)**[†]	2.11
3→4: $*O^{br}OH \to *O^{br}O + H^+(aq) + e^-$	-0.36(-0.69)	1.33
4→4A: $*O^{br}O + H_2O(l) + *O^{3c} \to O_2(g) + *O^{br}H + *O^{3c}H$	-0.83	-1.65
4A→1: $*O^{3c}H + H_2O(l) \to *H_2O + *O^{3c} + H^+(aq) + e^-$	0.42	2.02
w. vac.		
1→2: $*H_2O^t + *OH \to *O^tH + *OH + H^+(aq) + e^-$	**0.30(0.61)**	1.90
2→2A: $*O^tH + *OH + *O^{br} \to *OOH + *O^{br}H$	0.30(0.37)	0.23
2A→3: $*O^{br}H \to *O^{br} + H^+(aq) + e^-$	-0.04(-0.10)	1.54
3→4: $*OOH \to *OO + H^+(aq) + e^-$	-0.86(-0.71)	0.74
4→4A: $*OO + 2H_2O \to O_2(g) + *2H_2O$	0.05	-0.77
4A→1: $*2H_2O \to *H_2O^t + *OH + H^+(aq) + e^-$	0.25	1.85

[†] The bold free energy change indicates this step is rate-determining.

[‡] ΔE is the total energy change directly from DFT calculations at U = 0 V.

Crystal Structure for deprotonating β-NiOOH in VASP POSCAR format
```
    1.00000000000000
      4.7500428946883728    -0.0002042812318537     1.2912011403074222
     -0.0017070070714428    11.1933861817502880     0.0089177469502379
     -0.0978131021352734     0.0024159091574949     4.8161464890318424
   H    O    Ni
     2   16    8
Direct
  0.7549300147828117   0.4102729557502226   0.9467301216385814
  0.2550593160882023   0.7843243715444246   0.9466640894522479
  0.1496846218067820   0.0359771587822024   0.1922082227057922
  0.3864865734803069   0.0335534191833392   0.5948679825629418
  0.6496768580016923   0.1595374867930956   0.1922113484593065
  0.8865548647128566   0.1615891489710115   0.5953412222200493
```

0.1466712628110698   0.2830157047564382   0.1960089319491276
0.3938662507123157   0.2833247565064173   0.5897698812758992
0.6777926388451873   0.4099672206298389   0.1675934508885897
0.8576051943803308   0.4094149281215623   0.6120626728756677
0.1488083441987408   0.5358349884217332   0.1940956181784872
0.3924310524084003   0.5370218527648603   0.5923806629112444
0.6489916110881732   0.6595496053893553   0.1943052085539217
0.8927462744854979   0.6577183398274045   0.5923709006567554
0.1778669318379355   0.7849560073921026   0.1679240097120759
0.3577793984833769   0.7851053616924074   0.6122292774657254
0.6467400341943996   0.9124206322484806   0.1962855984658693
0.8938091845574219   0.9115443597276008   0.5898787604734611
0.7695369905703023   0.0351585136428185   0.3942441093178101
0.2695640080992372   0.1599706631070328   0.3940696867961422
0.7711467545430643   0.2832895960770654   0.3914093785283311
0.2657754583715093   0.4094155598133710   0.3961764973845949
0.7726291881711935   0.5364799940749740   0.3923572905648803
0.2727375935470320   0.6585230913635901   0.3923893802305855
0.7658777581178043   0.7855228913786306   0.3963782244814366
0.2713420118574787   0.9116777748296332   0.3914114875912812

Possible crystal Structure for γ-NiOOH intercalated with Na$^+$ and H$_2$O in VASP POSCAR format
   1.00000000000000
     4.7031640303783506   -0.0258657476331963   -1.1679762923942094
    -0.0441528411988384   8.3229426821574997   0.0092437910498497
    -0.0109505086100118   0.0077983583475757   7.0536847429025213
   H   O   Na   Ni
    8   16   2   6
Direct
  0.1760510777283476   0.6363304930566073   0.0331946987004005
  0.0832761910319634   0.6500702552376080   0.7965695151949252
  0.0858493796246537   0.2909822466762731   0.8077927095249732
  0.1568249435174024   0.2816314992110336   0.0379639197567959
  0.6720260401142543   0.0679236308696686   0.0442545789046594
  0.5977790576072728   0.0754418762882735   0.8093417997273589
  0.5982167666999844   0.4236565489277128   0.8095788729887163
  0.6367144506151322   0.4304123531153772   0.0401894252241684
  0.0997166409346254   0.7091275139707683   0.9221343240634327
  0.0158113876867456   0.2488806109195377   0.9180348020539345

0.5138326163081365   0.4651641950206298   0.9134272232227677
0.5755628405742150   0.7694025847853002   0.5699105408583899
0.0602543852610960   0.2702714209012655   0.5566345574453180
0.7600433365361489   0.7723258906487428   0.2742758901233526
0.3069931738880333   0.2612059533398005   0.2799194181702742
0.7934292215084837   0.1025374395389318   0.2811439457438137
0.2947664530670368   0.5976747061963261   0.2827312834011878
0.5552304623347294   0.1033587604208293   0.5623037184851150
0.0476957828395073   0.6097836933305938   0.5621976900048717
0.7770691746586963   0.4362870932671409   0.2786331640907082
0.5821411415468878   0.4319116126746904   0.5642931157607485
0.2890543513986980   0.9358021146460160   0.2826814286517013
0.0447370815547279   0.9432839398042769   0.5651517225816639
0.5960591084014468   0.0054241409011359   0.9224616997234696
0.1137119549476925   0.9802113191735684   0.9209390851149254
0.6141948525235298   0.7332189454333941   0.9204822438103699
0.6725384040040981   0.6037086441301309   0.4220024402438168
0.6777753873073512   0.2696622630937168   0.4206718377912072
0.1746149625630448   0.1022343468624206   0.4211078444492021
0.1684443449036982   0.7705709476263229   0.4222717922340652
0.1780322636097389   0.4358505525427278   0.4210596600436329
0.6704759548148398   0.9350779350802388   0.4227579783435471

References

1.   Li, Y.-F.; Selloni, A., Theoretical Study of Interfacial Electron Transfer from Reduced Anatase $TiO_2(101)$ to Adsorbed O_2. *J. Am. Chem. Soc.* **2013,** *135* (24), 9195-9199.

2.   Li, Y.-F.; Liu, Z.-P.; Liu, L.; Gao, W., Mechanism and Activity of Photocatalytic Oxygen Evolution on Titania Anatase in Aqueous Surroundings. *J. Am. Chem. Soc.* **2010,** *132* (37), 13008-13015.

3.   Li, Y.-F.; Selloni, A., Mechanism and Activity of Water Oxidation on Selected Surfaces of Pure and Fe-Doped NiO_x. *ACS Catal.* **2014,** *4* (4), 1148-1153.

4.   Li, Y.-F.; Liu, Z.-P., Structure and water oxidation activity of 3d metal oxides. *Wiley Interdisciplinary Reviews: Computational Molecular Science* **2016,** *6* (1), 47-64.

5.   Garcia-Mota, M.; Vojvodic, A.; Metiu, H.; Man, I. C.; Su, H.-Y.; Rossmeisl, J.; Nørskov, J. K., Tailoring the Activity for Oxygen Evolution Electrocatalysis on Rutile $TiO_2(110)$ by Transition-Metal Substitution. *ChemCatChem* **2011,** *3* (10), 1607-1611.

6.   Valdés, A.; Qu, Z. W.; Kroes, G. J.; Rossmeisl, J.; Nørskov, J. K., Oxidation and Photo-Oxidation of Water on TiO_2 Surface. *J. Phys. Chem. C* **2008,** *112* (26), 9872-9879.

7.   Bajdich, M.; García-Mota, M.; Vojvodic, A.; Nørskov, J. K.; Bell, A. T., Theoretical Investigation of the Activity of Cobalt Oxides for the Electrochemical Oxidation of Water. *J. Am. Chem. Soc.* **2013,** *135* (36), 13521-13530.

8.   Nørskov, J. K.; Rossmeisl, J.; Logadottir, A.; Lindqvist, L.; Kitchin, J. R.; Bligaard, T.; Jónsson,

H., Origin of the Overpotential for Oxygen Reduction at a Fuel-Cell Cathode. *J. Phys. Chem. B* **2004,** *108* (46), 17886-17892.